American Mineralogist, Volume 84, pages 37–47, 1999

Stability of high-Al titanite from low-pressure calcsilicates in light of fluid and host-rock composition

GREGOR MARKL* AND SANDRA PIAZOLO

Institut für Mineralogie, Petrologie und Geochemie, Albert-Ludwigs-Universität, Albertstrasse 23 b, D-79104 Freiburg, Germany

ABSTRACT

Titanite of variable Al and F content was found in granulite- to amphibolite-facies calcsilicates in Central Dronning Maud Land, Antarctica. The highest observed Al content corresponds to an X_{Al} [= Al/(Al + Ti)] of 0.53. Previously, such high values of X_{Al} were reported from high-pressure rocks, but the titanite of this study is from a low-pressure terrain. The compositional variations in titanite can be described for all samples by a set of three linearly independent exchange vectors added to the $CaTiSiO_5$ end-member titanite. In most rocks, these vectors are $Al_1F_1Ti_{-1}O_{-1}$, $Ti_{-0.25}\square_{0.25}O_{-1}OH_1$, and OH_1F_{-1}; in one sample, the $Ti_{-0.25}\square_{0.25}O_{-1}OH_1$ vector is replaced by a $Si_{-0.25}\square_{0.25}O_{-1}OH_1$ vector. The actual amount of exchange along these vectors and, therefore, the amount of Al in titanite, depends on *P* and *T*, on the composition of the coexisting fluid phase in terms of its H_2O/HF fugacity ratio, and on host rock composition in terms of Al_2O_3/TiO_2 activity ratio. It is inferred that, in suitable chemical environments, high-Al titanite is stable over a wide *P-T* range. Therefore, the Al content of titanite should not be used in geothermobarometry, even qualitatively. Additionally, because of the coupled substitutions $Al_1F_1Ti_{-1}O_{-1}$ and $Al_1OH_1Ti_{-1}O_{-1}$, the concentration of F in titanite is strongly dependent on the host rock chemistry. This rules out the easy use of titanite as a monitor of fluid composition.

INTRODUCTION

Titanite is a common mineral in a wide variety of rocks including calcsilicates, metabasites, and granitoid intrusives. Depending on the local chemical environment, titanite can incorporate variable amounts of elements like the REE, Mg, Na, Fe (both Fe^{2+} and Fe^{3+}), U, Th, Nb, Ta, or Sn (Ribbe 1982, and references therein). The most important substitution is that of Al for Ti, which is governed mainly by the exchange vectors $Ti_{-1}O_{-1}Al_1OH_1$ and $Ti_{-1}O_{-1}Al_1F_1$ (e.g., Ribbe 1982; Franz and Spear 1985; Enami et al. 1993; Carswell et al. 1996). Experiments by Smith (1981) showed that this exchange is dependent on pressure and that the maximum possible Al content of about 0.53 atoms per formula unit (apfu) is reached at pressures above 25 kbar in basaltic compositions (at 1200 °C). Oberti et al. (1991) suggested that the absence of An-rich plagioclase is crucial for the stabilization of high-Al titanite. Additionally, they showed that there is a positive correlation between Al and F content and decreasing Ca-O and octahedral cation-O bond lengths. Crystallographic reasons, however, cannot explain the apparent miscibility gap between the most aluminous titanite (with Al ~0.53 apfu) and the Ti-free, Al end-member vuagnatite [$CaAlSiO_4$(OH, F)].

Many of the known high-Al titanite occurrences are in high-pressure or even ultra-high-pressure rocks (Franz and Spear 1985; Carswell et al. 1996; Oberti 1991, and references therein). Nevertheless, the Al content of titanite must be governed by variables other than pressure, because Al-rich titanite also forms in low-pressure environments (e.g., in the Salton Sea geothermal system; Enami et al. 1993). Al-rich titanite, with Al contents up to 0.24 apfu, was also reported by Bernau and Franz (1987) from low-pressure calcsilicates where the incorporation of Al is governed mainly by the substitution of 2 Ti^{4+} = Nb^{5+} + Al^{3+}. Gibert et al. (1990) described titanite with up to 0.42 Al apfu in amphibolite-facies calcsilicates from the Montagne Noire, France, which formed at 4–5 kbar and 550–600 °C. In this case, the Al content appears to be controlled by the Al_2O_3/TiO_2 activity ratio in the host rocks and by the F content of the coexisting fluid. Carswell et al. (1996) also considered a high F activity to be responsible for the stabilization of titanite in ultra-high pressure rocks, where rutile-carbonate assemblages are expected to be stable at low F activity.

This short review demonstrates that highly aluminous titanite is found in rocks formed over the entire spectrum of geologically relevant pressure and temperature conditions. This paper presents an extensive set of data on titanite in calcsilicates from the medium-pressure granulite- to amphibolite-facies area of Central Dronning Maud Land (CDML), Antarctica. We focus on the effects that chemical variations in the coexisting fluid phase and in the host rock have on the composition of titanite.

* E-mail: markl@ruf.uni-freiburg.de

0003–004X/99/0102–0037$05.00

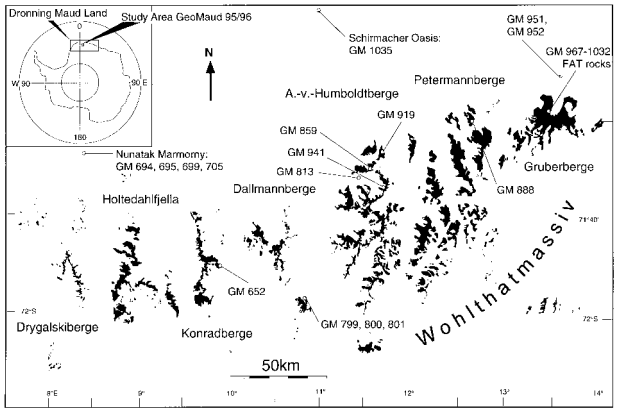

FIGURE 1. Map of the study area in Central Dronning Maud Land, Antarctica, with sample localities indicated (see Appendix A).

GEOLOGICAL SETTING

The area of the present study lies within the East Antarctic craton. The German GeoMaud expedition 1995 to1996 found large areas of mainly undeformed felsic and less-common basic intrusives, including older anorthosites and gabbros, and younger pyroxene- and fayalite-bearing charnockites (Markl and Henjes-Kunst 1999). Anorthosites occur as two complexes associated with gabbroic and noritic rocks: a large complex in the Gruberberge and a smaller one in the northern A.-v.-Humboldtberge (Fig. 1). The magmatic rocks intruded into a basement consisting of metagranitoids and migmatites (~25%), a bimodal sequence of presumably metavolcanic rocks (~15%), and a supracrustal series of metapelitic Grt-Sil-Bt schists (~10%) and calcsilicates that are commonly associated with Fo-Spl marbles (~1%; mineral abbreviations after Kretz 1983). The calcsilicates and marbles occur as layers between 10 cm and several meters thick, which can be traced for up to 200 meters, and as lenses one to several meters long. The inner parts of the lenses consist of Fo-Phl-Spl marble that grades into Di-bearing marble and finally into Wo-Scp-Di-Grt-Phl±An±Kfs±Ttn-bearing calcsilicate at the contacts with surrounding gneisses.

Two main regional tectonometamorphic events can be distinguished: an older Grenvillian orogeny at roughly 1.1–1.0 Ga and a younger Panafrican event at 500–600 Ma (Jacobs et al. 1998). Throughout the entire region, the Panafrican event strongly overprints the structures and metamorphic textures of the Grenvillian orogeny (Dalziel 1991; Jacobs et al. 1998). The metamorphic conditions during the Panafrican event appear to have been fairly homogeneous throughout the study area. As shown in Figure 2a, metamorphic conditions during this event in CDML are estimated to have reached granulite facies conditions of ~830 °C and 7 kb (Rao et al. 1997; Piazolo and Markl 1999). Subsequent Panafrican amphibolite facies retrogression occurred in two stages at ~650 °C and 4.5 ± 0.5 kb and as ~490 ± 20 °C and 3 ± 1 kb (Rao et al. 1997; Piazolo and Markl 1999; Andrehs and Bormann 1995). The last stage at lower amphibolite facies conditions is indicated only by margarite-bearing coronas in a few calcsilicate samples.

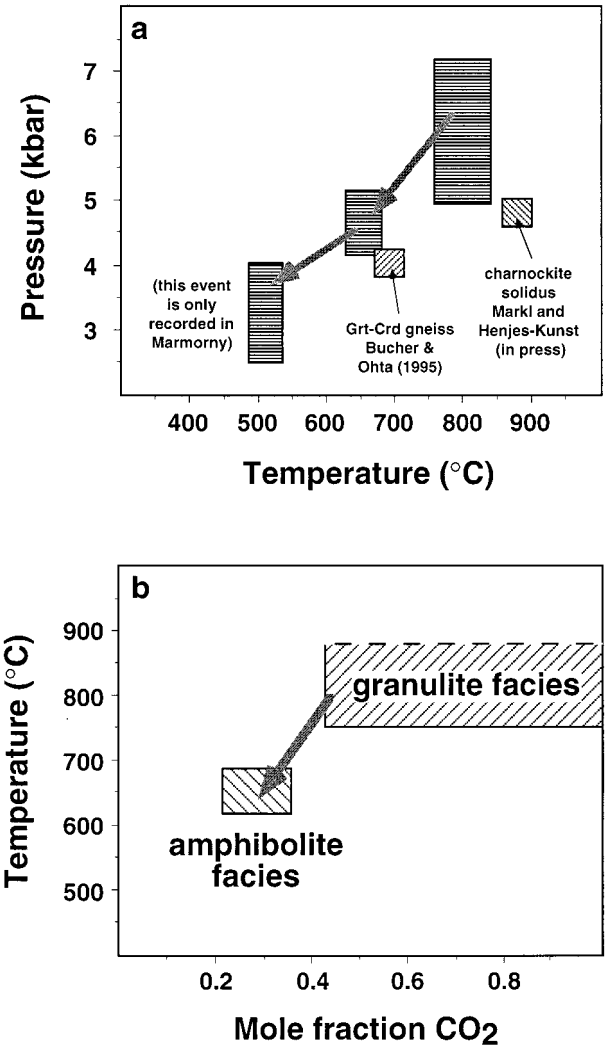

FIGURE 2. (**a**) *P-T* diagram showing the estimates for peak granulite-facies metamorphism and for amphibolite-facies retrogression [after Rao et al. (1997) and Piazolo and Markl (1999)]; (**b**). *T*-X_{CO_2} diagram relating peak granulite-facies metamorphism to CO_2-rich, amphibolite-facies retrogression to CO_2-poor fluid compositions (after Piazolo and Markl 1999). The boxes in A and B are based on phase equilibria involving the mineral phases Scp, Wo, Cc, Qtz, An, Cpx, and Grt. They show the whole range in fluid compositions (**b**) observed in the various samples.

In the calcsilicates, the transition from granulite- to amphibolite-facies conditions is reflected by the change from early Wo-Di-Scp-Ttn to later Grt-Qtz-Cal-Ttn assemblages. This change is accompanied by a considerable shift from CO_2-rich fluid compositions (from X_{CO_2} ~0.45 in Wo-bearing samples to X_{CO_2}>0.56 in scapolite-bearing samples) under granulite-facies conditions to more H_2O-rich fluid compositions (X_{CO_2} = 0.23–0.30) under am-

TABLE 1. Mineral assemblages in the calcsilicate samples used in this study (with the exception of the FAT-rock samples)

Sample no.	Locality	Mountain range	Equilibrium assemblages with titanite (modes)	Other assemblages (modes)	Conditions of equilibrium inferred from textures
GM 652	SE Sandhø	Konradberge	Amph (20%), Phl (15%), Ttn (5%), Fl (2%)	Scp (35%), Qtz (10%), Cal (7%), Ilm (<1%)	amphibolite facies
GM 694		nunatak Marmorny	(1) Cpx (70%), Kfs (5%), Amph (5%), Ttn (3%) (2) Amph (10%), Phl (8%), Ttn (3%)		(1) granulite facies (2) amphibolite facies
GM 695		nunatak Marmorny	Phl (25%), Ttn (3%)	Spl (30%), Cpx (25%), An (10%)	amphibolite facies
GM 699		nunatak Marmorny	Phl (20%), Amph (10%), Qtz (5%), Ttn (3%)	Cpx (50%), An (5%)	amphibolite facies
GM 705		nunatak Marmorny	Amph (5%), Ttn (5%), An (5%)	Cpx (75%), Ilm (5%), Ap (5%)	amphibolite facies
GM 799		Gjeruldsenhøgda	(1) Cpx (30%), Scp (30%), Wo (20%), Ttn (3%) (2) Grt (8%), Cal (3%), Qtz (3%), Ttn (3%)		(1) granulite facies (2) amphibolite facies
GM 800		Gjeruldenhøgda	Grt (10%), Qtz (7%), Ttn (3%), Cal (5%), Kfs (5%)	Cpx (25%), Scp (25%), Wo (20%)	amphibolite facies
GM 801		Gjeruldsenhøgda	Grt (15%), Cal (4%), Qtz (4%), Ttn (3%)	Scp (30%), Wo (25%), Cpx (20%)	amphibolite facies
GM 813	Schüssel moraine	Humboldtberge	Amph (32%), An (10%), Phl (5%), Ttn (2%)	Cpx (17%), Spl (10%), Grt (10%)	amphibolite facies
GM 859	Eckhörner (east)	Humboldtberge	Cpx (15%), Wo (13%), Scp (12%), Ttn (5%)	Cal (35%), Qtz (10%), Kfs (10%)	granulite facies
GM 888	Mt. Aerodromnaya	Petermannberge	An (35%), Cpx (30%), Wo (25%), Ttn (10%), Qtz (7%)		granulite facies
GM 919	NE-ridge of Insel	Humboldtberge	Cpx (30%), Grt (30%), Gr (8%), Kfs (7%), Ttn (4%)	Amph (10%), An (10%)	granulite facies
GM 941	Ridge S Überlauf	Humboldtberge	Grt (40%), Qtz (10%), Cal (7%), Ttn (3%)	Cpx (25%), Wo (8%), Scp (5%)	amphibolite facies
GM 951		nunatak Odrodnaya	Cpx (25%), Qtz (20%), An (15%), Cal (10%), Scp (10%), Ttn (3%)	Grt (15%)	granulite facies
GM 952		nunatak Odrodnaya	Cpx (30%), An (20%), Scp (15%), Ttn (10%), Qtz (5%), Wo (5%), Cal (3%)	Grt (5%)	granulite facies
GM 1035	Lake Sbrosovoje	Schirmacher Oasis	Grt (35%), Qtz (10%), Cal (8%), Ttn (5%)	Cpx (15%), Wo (8%), Scp (8%), An (5%)	amphibolite facies

Note: Mineral abbreviations according to Kretz (1983).

phibolite-facies conditions (Fig. 2b; Piazolo and Markl 1999). The granulite facies metamorphism predates the intrusion of large amounts of charnockitic magma that released fluids and triggered the amphibolite-facies retrogression in the country rocks at ~650 °C and 4.8 ± 0.3 kb (Bucher and Ohta 1993; Markl and Henjes-Kunst 1999; Markl and Piazolo 1998). Retrogression is not pervasive throughout most of the area, suggesting that the fluid influx was limited (see also Markl and Piazolo 1998).

SAMPLE DESCRIPTIONS

Sample localities and field relations

Figure 1 shows the sample localities, which are described in detail in Appendix A. All samples are calcsilicates, but from different environments. Most are regionally metamorphosed rocks (GM 652, 694, 695, 699, 705, 799, 800, 801, 813, 888, 919, 941, 951, 952, 1035) but a few are xenoliths in charnockites (GM 859) and ferrodiorites (GM 967–1032, ''FAT rocks''). The FAT rocks are distinctive because titanite locally comprises up to 100% of the rock on a scale of several decimeters or even meters. In all other calcsilicate samples, titanite is a minor constituent and occurs as small euhedral to anhedral grains up to 2 mm in size.

Available thermobarometry data (Piazolo and Markl 1999) suggest that most samples were subjected to similar *P-T* conditions during the Panafrican metamorphism. The xenoliths, however, occur in mostly unretrogressed rocks and do not show features of later deformation or metamorphic overprint. Hence, they may record contact metamorphic temperatures in the range 850–950 °C. Temperature estimates (Piazolo and Markl 1999) indicate minimum values of 770 °C. Thus, the titanite in all samples appears to have equilibrated under amphibolite- or granulite-facies conditions.

Description and interpretation of microtextures

Table 1 provides mineralogical data for each particular sample. A few samples are described in detail below to highlight both the special characteristics and the typical textural variations of the calcsilicates.

Sample GM 652. The sample is composed of scapolite, phlogopite, and amphibole, with minor amounts of titanite (Fig. 3a), fluorite, quartz, calcite, ilmenite, apatite, and zircon. Sample GM 652 is the only one that contains fluorite, which forms grains several millimeters in size, found in stable association with titanite, biotite, and amphibole (Fig. 3b). Scapolite forms large crystals (1–3 mm) with relict calcite as inclusions. In scapolite-domi-

nated areas, quartz occurs in equilibrium with calcite. Titanite occurs as aggregates of anhedral crystals surrounding tiny grains of earlier ilmenite in the calcite-quartz matrix.

This sample was collected close to a body of charnockite. Because the charnockites in the area are generally very rich in F (some even reached fluorite saturation; Markl and Piazolo 1998), we interpret the titanite, biotite, and amphibole as having formed during reaction of a precursor, ilmenite-bearing calcsilicate with F-rich fluids released from the charnockite during the amphibolite-facies overprint at about 650 °C.

Sample GM 694. In this sample, large flakes of calcic amphibole ~2 mm across occur in a homogeneous matrix of clinopyroxene. Based on color and composition, two generations of calcic amphibole are present: an earlier, dark green, Fe-rich type and a later, lighter green, Fe-poor variety. Biotite is common as small isolated grains (~1 mm) and, in some cases, it forms rims on potassium feldspar; some grains are altered to chlorite.

Titanite with slightly arcuate grain boundaries can be found throughout the whole section. Microprobe analyses and backscattered electron (BSE) images reveal two generations of titanite (see Tables 1 and 2, and Fig. 3c). Although it is not possible to determine which variety is earlier, we interpret one to have formed under granulite-, and the other under upper amphibolite-facies conditions. Based on the comparison with sample GM 652, we infer that the titanite with the higher contents of F and Al formed under amphibolite-facies conditions. Zircon, anorthite, and zoisite are present in small amounts throughout the thin section.

Sample GM 799. In this sample, garnet formed by a reaction of scapolite with wollastonite and clinopyroxene. In garnet-free zones, clinopyroxene occurs as small grains in stable association with scapolite and wollastonite. In garnet-bearing parts of the sample, quartz is stable with calcite. Nevertheless, wollastonite grains are commonly unaltered and only decompose to calcite and quartz in close proximity to garnet. Because the garnet-forming reaction liberates CO_2 and thereby triggers wollastonite decomposition to calcite and quartz (Piazolo and Markl 1999), this texture indicates very local buffering of the fluid composition. Some wollastonite encloses grains of calcite. Titanite is stable throughout the rock in all assemblages representing both granulite and upper amphibolite facies conditions.

Sample GM 888. This sample does not show any modal zonation or retrogression. Wollastonite is present in small (0.5 mm) to large (3 mm) grains in stable association with clinopyroxene and abundant anorthite. Quartz and very small amounts of calcite are present, and appear to represent a stable assemblage. Accessory titanite and apatite are rounded to amoeboid, and are interpreted to have formed under granulite-facies conditions.

Sample GM 951. Clinopyroxene and anorthite form the matrix of this thin section. Scapolite commonly contains anorthite in its core. Clinopyroxene-scapolite, scapolite-quartz, and calcite-quartz are stable assemblages. Where garnet is present, scapolite and clinopyroxene are found only as relicts and inclusions in garnet. Titanite is mostly euhedral, showing its typical spear-like shape. It was stable with clinopyroxene, scapolite, anorthite, calcite, and quartz as well as with scapolite. Based on textures of these minerals, the titanite is interpreted to have formed during the granulite-facies event.

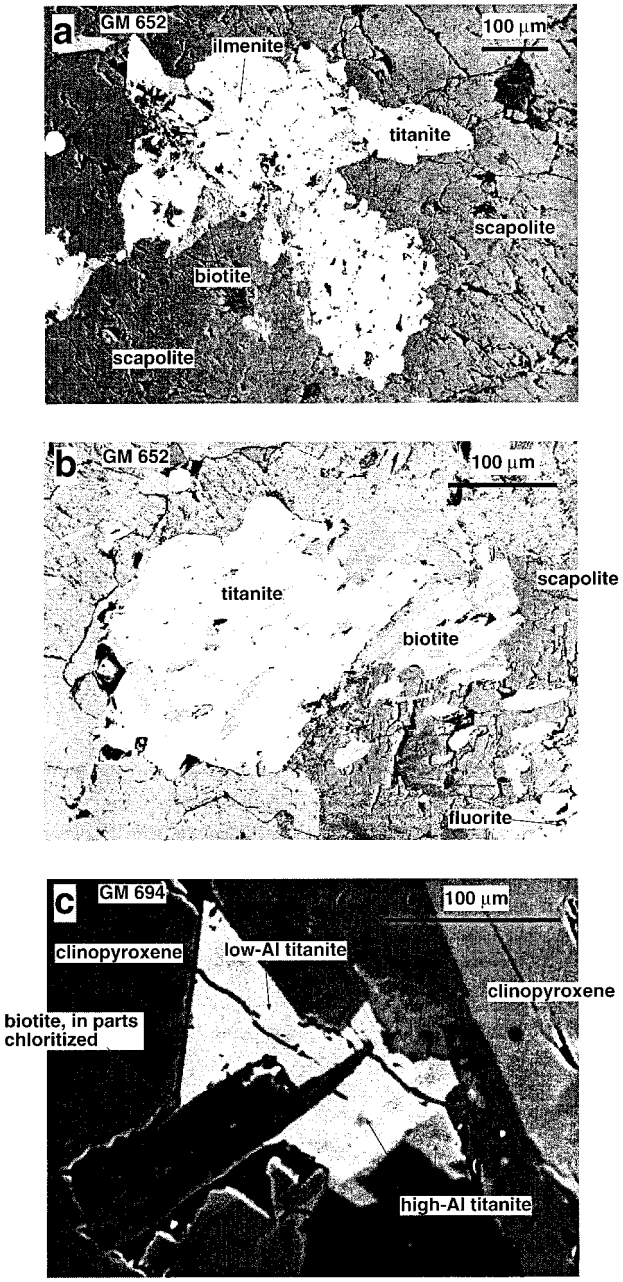

FIGURE 3. BSE images of textures observed in Dronning Maud Land calcsilicates. (**a** and **b**) Textures in sample GM 652; (**c**) Textures in sample GM 694. Note the slight gray contrast between high-Al and low-Al titanite in this sample.

GM 967–1032. These samples contain only feldspars, augite, and titanite (for which reason we call them FAT rocks), which are in textural equilibrium. They show no relicts of earlier assemblages and no retrogressive overprint, but both augite and plagioclase exhibit significant compositional zonation. Plagioclase rarely shows fine-grained exsolutions of potassium feldspar, but large potassium feldspar grains are devoid of plagioclase exsolutions. We interpret these features as the result of diffusive re-equilibration, whereas the overall mineral assemblage still represents the conditions under which the xenolith recrystallized in the ferrodioritic magma.

Mineral chemistry

Analytical techniques

Microprobe analyses were performed on a Cameca SX100 with 5 WDS spectrometers at the Universität Freiburg. The samples were calibrated against synthetic and natural standards supplied by Cameca. Fluorine was calibrated on a MYCALEX F-phlogopite containing 9.41 wt% F. Analytical conditions were 10 nA and 15 kV, with counting times of 20 s for all elements except F, which was measured for 60 s. Raw data were processed by procedures described in Pouchou and Pichior (1984). Uncertainties for all elements are estimated to be about ±5% (relative), and detection limits are ~0.1 wt%.

Titanite

Analytical data and correlations. Table 2 lists representative microprobe analyses of titanite. Weak zoning was detected only in titanite from some samples of FAT rocks. Mg, Mn, and Cl are present in amounts below 0.1 wt%. Reconnaissance measurements for other elements (Na, REE) also revealed concentrations below 0.1%. Calcium values ranged between 0.98 and 1 apfu. For Mg, Na, Mn, Cl, and Ca, no clear correlation with any other element could be detected. Interestingly, the titanites coexisting with fluorite in sample GM 652 do not show the highest F content, which is found in sample GM 694.

Figure 4 shows the compositional variation of titanite from various samples relative to its F or (F + OH) content. Vacancies calculated after the method of Oberti et al. (1991; see below), are always ≤0.02 per formula unit (pfu) with the exception of the samples from the FAT rocks, where a clear correlation exists among Si, vacancies, and (F + OH) (Fig. 4a). In all other samples, Si is uncorrelated with (F + OH). Ti is strongly correlated with (F + OH), but the trends vary in detail: the FAT rocks show the weakest and GM 694 the strongest correlation, and the rest of the calcsilicates plots within an intermediate range as a relatively homogeneous group (Fig. 4b). The same holds true for Al against (F + OH), where GM 694 shows a strong, the rest of the calcsilicates a good, and the FAT rocks virtually no correlation (Fig. 4c). Because F is correlated almost perfectly with Al (Fig. 4d), these differences in (F + OH)-Al correlation can be explained by differences in OH substitution. This is corroborated by the F vs. (F + OH) plot (Fig. 4e), where it is obvious that F and OH behave differently in different samples, but consistently within one sample or sample group. In contrast to pegmatitic environments (e.g., Černý et al. 1995), exchanges involving Ca were not observed in the Antarctic rocks because Ca is buffered in the calcsilicate host rocks.

Formula calculation. The formulae were calculated according to the procedure described in Oberti et al. (1991), which assumes full occupancy of the Ca, Si, and Ti sites, and that all Fe is present as Fe^{3+}. If vacancies remain on these sites following the calculation procedure, then several reasons can be responsible (Oberti et al. 1991): (1) vacancies are actually present; (2) analytical error; (3) the assumption that all Fe is present as Fe^{3+} is incorrect; and (4) additional elements are present that were not analyzed. Hence, an imperfect analysis will typically result in calculated vacancies. We tested the effect of (3) by calculating the most Fe-rich analysis with $Fe_{tot} = Fe^{3+}$ and then with $Fe_{tot} = Fe^{2+}$. There was only a minimal difference in the calculated number of vacancies (<1% relative) and the only differences were deviations in the calculated OH/O ratio (~2% relative), which are smaller than the analytical uncertainty. Because the calculated Ca was always between 0.98 and 1 apfu, caveat (2) was not assumed to be of great importance. If analytical uncertainties or the formula calculation procedure created artificial vacancies or other errors, the observed sample-dependent behavior would not be expected. We conclude therefore that calculated vacancies >0.02 pfu, especially those that are correlated with other changes in stoichiometry (see below), do represent real vacancies.

Biotite

Biotite from the calcsilicate rocks ranges in composition from virtually pure phlogopite to types with up to 35% annite and 20% siderophyllite component. Fe and Al are roughly correlated. The F content is highly variable and, as Figure 5a demonstrates, it is not noticeably correlated to X_{Fe} of the biotite. There is, however, a correlation with Al in sample GM 652 (Fig. 5b).

Clinopyroxene

In the FAT rocks, clinopyroxene is strongly zoned: from core to rim, Al, Na, Ti, and Fe^{2+} decrease, whereas Mg, Fe^{3+}, and Ca increase. Values of X_{Fe} fall in the range 0.42–0.61. Clinopyroxenes in the rest of the calcsilicate samples range in composition from pure diopside to pure hedenbergite. Al contents are very low, typically <0.1 apfu, reaching values of 0.2 apfu in only two analyses.

Garnet

Generally, the garnet is a pure grossular or a binary grossular-andradite solid solution with only small amounts of almandine. The garnet in sample GM 813, however, is an andradite-poor grossular-almandine solid-solution with a composition of $Alm_{60–80}Grs_{40–20}$. The sample occurs at the margin of a calcsilicate lens near its

TABLE 2. Selected microprobe analyses of titanite from calcsilicates and FAT rocks from Dronning Maud Land, Antarctica

Mineral no.	652-5	652-7	652-8	652-19	694-35	694-56	694-38	694-40	694-41
wt%									
SiO_2	30.84	30.44	33.79	31.41	31.08	31.38	31.85	31.05	31.36
TiO_2	31.86	28.36	23.76	26.95	28.33	21.34	18.78	26.12	25.10
Al_2O_3	5.84	7.99	11.54	9.62	7.58	12.40	14.29	9.52	10.61
FeO	0.39	0.47	0.48	0.42	0.35	0.30	0.23	0.25	0.31
MnO	ND	ND	ND	ND	0.03	0.01	0.05	0.05	0.07
MgO	0.05	0.21	0.13	0.11	0.02	0.00	0.02	0.04	0.03
CaO	28.48	26.89	25.50	28.81	29.28	29.76	30.23	29.49	29.73
Na_2O	0.00	0.03	0.43	0.02	0.00	0.00	0.00	0.00	0.00
K_2O	ND	ND	ND	ND	0.03	0.01	0.04	0.03	0.03
Cl	ND	ND	ND	ND	0.00	0.01	0.00	0.01	0.00
F	2.24	2.94	3.04	3.74	3.09	4.73	5.76	3.71	4.01
Total corrected for F, Cl	98.80	96.16	97.45	99.55	98.52	97.99	98.85	98.73	99.58
Formula proportions*									
Ti	0.77	0.69	0.53	0.64	0.68	0.50	0.44	0.62	0.59
Al	0.22	0.31	0.40	0.36	0.29	0.46	0.05	0.36	0.39
Fe^{3+}	0.01	0.01	0.01	0.01	0.09	0.08	0.06	0.07	0.08
Si	0.99	0.99	1.00	0.99	0.99	0.98	0.98	0.98	0.99
Ca	0.98	0.94	0.81	0.97	0.01	0.01	0.01	0.01	0.01
O	4.74	4.55	3.98	4.58	4.06	4.03	4.03	4.05	4.05
CH	0.03	0.13	0.71	0.03	0.11	0.02	0.14	0.11	0.71
F	0.23	0.32	0.32	0.39	0.33	0.50	0.61	0.39	0.42

Note: ND = not detected.
* Calculated after Oberti et al. (1991), all Fe as Fe^{3+}, some minor elements excluded.

contact with the enclosing gneiss. Pyrope and spessartine are insignificant in abundance in all garnets.

Feldspars

Plagioclase is present in a few calcsilicate samples, in some cases as an early phase, and in others as a late breakdown product of scapolite. Most plagioclase compositions are between An_{90} and An_{100}, but two samples (GM 813 and 1035) contain a more sodic plagioclase (up to An_{55}). Potassium feldspar (Or_{90-100}) also occurs in a few calcsilicate samples. In the FAT rocks, small (≈0.5 mm), unzoned plagioclase grains (An_{30} and An_{85}) are associated with potassium feldspar of composition Or_{90}. The variation of X_{An} reflects the compositional zonation of the xenoliths, with the most Ca-rich plagioclase found in the core of individual xenoliths. All of these feldspar types coexist with titanite in some samples.

DISCUSSION

Exchange vectors

In our discussion, we begin with a consideration of the FAT rocks before discussing the more heterogeneous calcsilicate group. Titanite in the FAT rocks show substitutions related to Si and OH, but not to Al or F (Figs. 4c, 4d, and 4e) nor to Fe. Keeping charge balance and site occupancy in mind, this effectively constrains the governing exchange mechanism to the vector

$$\square_{0.25}OH_1Si_{-0.25}O_{-1}. \quad (1)$$

Al and F in the FAT rocks are well correlated (Fig. 4d), which can be explained by the well-known vector

$$Al_1F_1Ti_{-1}O_{-1}. \quad (2)$$

For a complete description of titanite compositions, the minor exchange vectors

$$\square_{0.25}F_1Si_{-0.25}O_{-1} \quad (3)$$

and

$$Al_1OH_1Ti_{-1}O_{-1} \quad (4)$$

must also be considered.

Because these four vectors are not linearly independent, just Equations 1 and 2 can be used in combination with the simple exchange

$$OH_1F_{-1} \quad (5)$$

to describe the complete observed compositional variation of titanite in the FAT rocks. If this is so, then all measured compositions must be a linear combination of these three vectors.

The magnitudes of the various exchange vectors can be determined by a least-squares fit to the equation

$$A + x*(1) + y*(2) + z*(5) = B$$

where A is a vector describing the end-member titanite composition (i.e., the additive component), x, y, and z are the calculated magnitudes of the exchange vectors 1, 2, and 5, and B is the measured titanite composition. If the vectors 1, 2, and 5 are appropriate and sufficient to describe the observed compositional variations of the titanites, a plot of measured vs. calculated (i.e., the calculated magnitudes of the exchange vectors applied to the end-member titanite composition) titanite compositions should give a 1:1 line. This is indeed almost perfectly the case for the FAT rock titanites (Fig. 6).

The same procedure for the rest of the calcsilicate sam-

TABLE 2.—*Extended*

Mineral no.	967-2	967-4	967-13	967-14	967-23	1013-5	1013-6	1013-34
wt%								
SiO_2	30.30	30.54	29.57	27.73	28.19	28.55	29.39	28.85
TiO_2	33.54	33.77	34.57	33.71	33.73	33.82	34.96	33.84
Al_2O_3	4.70	4.58	4.08	4.51	4.44	4.50	4.24	4.53
FeO	1.10	1.06	1.02	0.95	0.99	0.93	1.10	1.18
MnO	0.06	0.02	0.06	0.02	0.04	0.01	0.04	0.03
MgO	0.00	0.00	0.00	0.00	0.00	0.00	0.00	0.00
CaO	29.06	28.85	28.97	29.22	29.15	29.06	29.21	29.22
Na_2O	0.00	0.01	0.02	0.01	0.01	0.00	0.00	0.00
K_2O	0.01	0.00	0.00	0.01	0.00	0.00	0.01	0.02
Cl	0.00	0.01	0.00	0.00	0.01	0.02	0.00	0.00
F	1.96	1.85	1.61	1.86	1.81	1.77	1.68	1.77
Total corrected for F, Cl	100.02	100.01	99.31	97.32	97.69	98.00	100.04	98.80
Formula proportions								
Ti	0.81	0.82	0.84	0.81	0.81	0.82	0.84	0.81
Al	0.18	0.17	0.15	0.17	0.17	0.17	0.16	0.17
Fe^{3+}	0.03	0.03	0.03	0.03	0.03	0.03	0.03	0.03
Si	0.97	0.98	0.95	0.89	0.90	0.92	0.94	0.92
Ca	1.00	0.99	1.00	1.00	1.00	1.00	1.00	1.00
F	0.20	0.19	0.17	0.20	0.19	0.19	0.17	0.19
CH	0.04	0.02	0.12	0.43	0.37	0.29	0.14	0.27
O	4.75	4.79	4.71	4.37	4.44	4.52	4.68	4.54

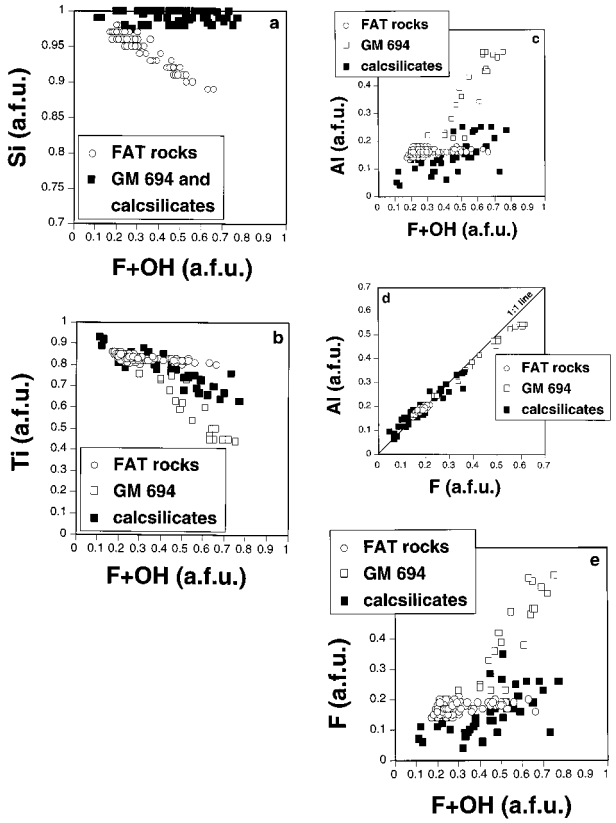

FIGURE 4. Correlations between various elements and F or (F + OH) in titanites from Dronning Maud Land (in atoms per formula unit).

ples reveals that the same set of exchange vectors (vectors 1, 2, and 5) cannot describe their compositional variations. This is, for example, demonstrated by the plot for Si in Figure 6, where the results for the calcsilicate samples strongly deviate from the 1:1 line. Here, the compositional dependencies imply that the vector

$$\square_{0.25}OH_1Ti_{-0.25}O_{-1} \quad (6)$$

is of importance. This vector is responsible for variations in OH content unrelated to variations in Al content. If vector 1 is replaced by vector 6, the compositional variations of the calcsilicate titanites can be reproduced almost perfectly in the way detailed above for the FAT rocks. In our samples, the type of exchange involving vacancies (vectors 1 and 3) favors OH over F, whereas F is strongly preferred over OH for the coupled exchange involving Al (vectors 2 and 4). The lack of Al-F correlation in the samples described by Gibert et al. (1990) indicates, however, that this statement is not necessarily true for other areas.

Only the FAT rock titanite exhibits the effect of exchange vector 1. Because the FAT rock samples are texturally different from the calc-silicate samples, we con-

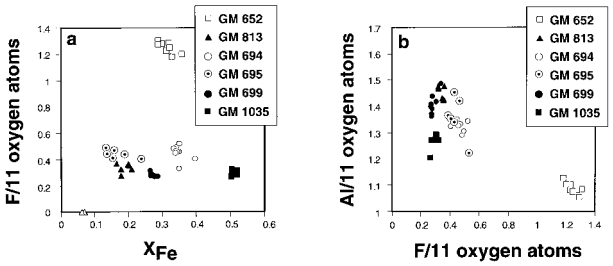

FIGURE 5. Correlation between F, X_{Fe}, and Al in biotites from Central Dronning Maud Land (in atoms per formula unit).

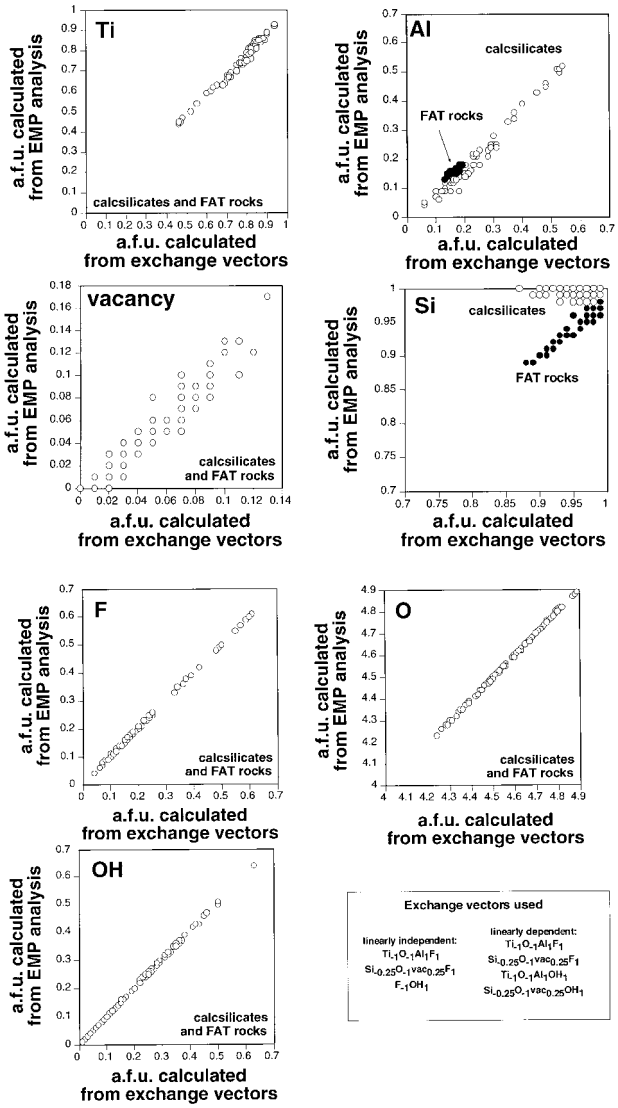

FIGURE 6. Diagrams of atoms per formula unit as calculated from microprobe analyses against atoms per formula units as calculated from a linear combination of exchange vectors (see text for details).

clude that the contact-metamorphic effect and the possible interaction with the ferrodioritic melt favored the hydroxylation process governed by vector 1 whereas, in the rest of the samples, vector 6 was involved.

The role of vacancies in titanite

Ribbe (1982) states, that there is ''no significant evidence for non-stoichiometry in titanite.'' However, Rosenberg (1974) found that, with decreasing temperature, the substitution

$$\square + 4H^{+} = Si^{4+} \quad (7)$$

(a different notation for our vector 1), is observed in synthetic titanite. The FAT rock samples therefore appear to provide the first reported natural evidence for this hydroxylation mechanism. Additionally, Černý et al. (1995) reported a substitution mechanism involving vacancies for extremely Ta- and Nb-rich titanite. We conclude therefore that the occurrence of vacancies in titanite may be more common—though always limited—than previously suggested. Mismatches in cation sums previously assigned to analytical difficulties may in fact be caused by the presence of vacancies.

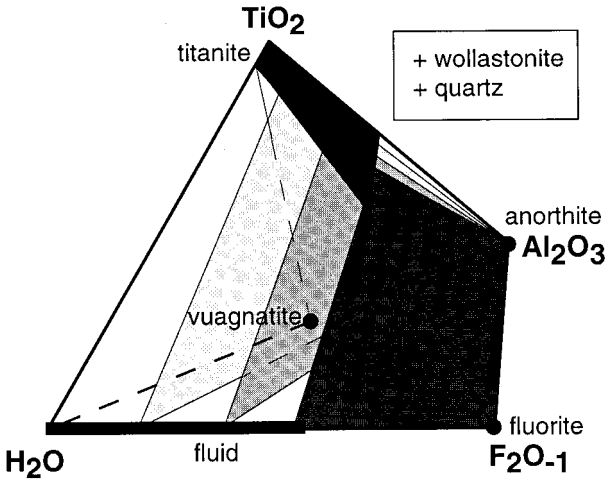

FIGURE 7. TiO_2-H_2O-F_2O_{-1}-Al_2O_3 tetrahedron describing schematically the phase relations among titanite of variable composition, anorthite, vuagnatite, fluorite, and an H_2O-HF fluid in assemblages with wollastonite and quartz.

The importance of fluid and rock compositional variables

Exchange vectors involving Ca were reported by Černý et al. (1995), but were not observed in our samples. We infer that this is an effect of the host rock composition, which is Ca-rich in our samples but Ca-poor (pegmatitic) in the samples described by Černý et al. (1995). Furthermore, we have shown above that, if the FAT rocks are excluded, three exchange vectors (2, 5, and 6) are sufficient to describe the compositional variations of titanite in the Antarctic calcsilicates. Intuitively, these vectors appear to be dependent on Al_2O_3 activity, on TiO_2 activity, or on HF fugacity, and thus governed by the local rock composition and by a variable related to fluid composition.

Carswell et al. (1996) pointed out that the Al content of titanite is dependent not only on *P* and *T*, but also on the activity of F relative to CO_2 because of equilibria involving rutile and carbonate. Gibert et al. (1990) showed the dependence of titanite composition on TiO_2 and Al_2O_3 activity in addition to F activity. The schematic diagram of Figure 7 shows the importance of the composition of an H_2O-HF fluid on titanite composition in wollastonite-, anorthite-, and quartz-bearing calcsilicates. In general, F-rich titanite would coexist with fluorite and high-F fluids, titanite of intermediate F content would coexist with an

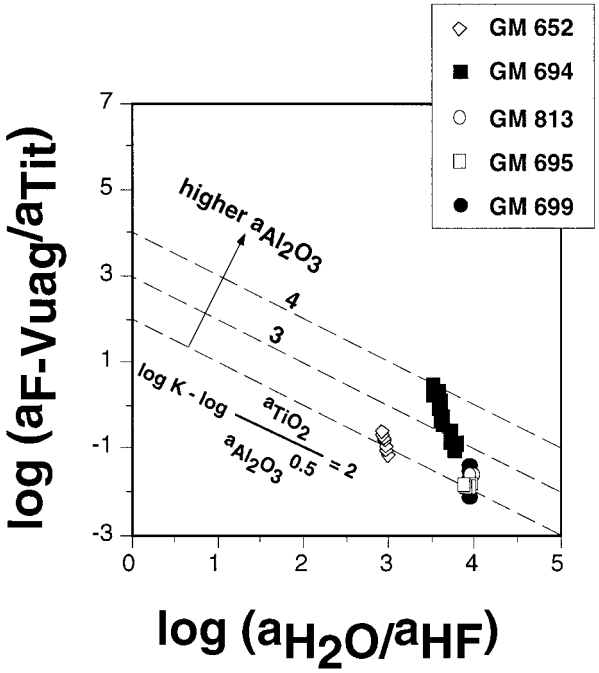

FIGURE 8. Diagram of $\log(a_{H_2O}/a_{HF})$ calculated from coexisting biotite vs. $\log(a_{F-Vuag}/a_{Ttn})$ and with contour lines for logK-log $(a_{TiO_2}/a_{Al_2O_3}^{0.5})$. Note that the fluorite-bearing sample GM 652 plots at fluid compositions significantly different from the other calcsilicate samples, but it shows similar logK-log $(a_{TiO_2}/a_{Al_2O_3}^{0.5})$ values. For discussion and further explanation see text. (F-Vuag = the hypothetical F-bearing vuagnatite.)

intermediate fluid, and OH-rich titanite is expected to coexist with vuagnatite and anorthite or with vuagnatite and a pure H_2O-fluid.

To test these predictions, we determined H_2O/HF fugacity ratios in the fluid coexisting with biotite after the method of Munoz and Swenson (1981) at a temperature of 750 °C for samples in which titanite coexists with biotite (GM 652, 694, 695, 699, and 813). We found that because of the coupling of Al and F substitution in titanite, the simple exchange reaction

$$CaAl_xTi_{1-x}SiO_{5-x}OH_x + xHF = CaAl_xTi_{1-x}SiO_{5-x}F_x + xH_2O,$$

(which is essentially exchange vector 5), is not sufficient to relate the F content of titanite and the f_{H_2O}/f_{HF} ratio of the fluid. Exchange vector 5 is able to describe the compositional variations, but it does not refer to a process actually observed in nature. This is highlighted by the fact that the titanite in GM 652, which coexists with fluorite, does not have the highest F content. The alternative explanation, that the titanite and the biotite in this sample are in disequilibrium, is not supported by the observed textures (Figs. 3a and 3b).

However, if one considers the reaction

$$CaTiSiO_5\ (Ttn) + 0.5Al_2O_3 + HF = CaAlSiO_4F\ (F - Vuag) + TiO_2 + 0.5H_2O,$$

which is a representation of vector 2, the F-Vuag/Ttn activity ratio is dependent on fluid composition, *P*, *T*, and variables determined by rock chemistry. Here, the mineral composition is related to the fluid composition via the equation

$$\log(a_{F-Vuag}/a_{Ttn}) = \log K - \log(a_{TiO_2}/a_{Al_2O_3}^{0.5} - \log a_{H_2O}^{0.5}/a_{HF}).$$

In Figure 8, our results are plotted in a $\log(a_{F-Vuag}/a_{Ttn})$ vs. $\log(a_{H_2O}/a_{HF})$ diagram. Assuming constant *P* and *T*, an ideal solution model for F and Al in titanite, and under the assumption that $\log(a_{H_2O}/a_{HF}) \approx \log(a_{H_2O}^{0.5}/a_{HF})$ (which produces small errors in H_2O-rich fluids), titanites that formed at constant *P*, *T*, and $(a_{TiO_2}/a_{Al_2O_3}^{0.5})$ activity ratios would lie on one of the dashed lines, depending on the fluid chemistry. Most of the observed titanite compositions form a single trend oblique to these lines and therefore (keeping the aforementioned caveats in mind) indicate changes in the TiO_2/Al_2O_3 activity ratio rather than changes in fluid chemistry as responsible for the observed compositional variations in these samples. The fluorite-bearing sample GM 652, however, shows considerably lower H_2O/HF fugacity ratios at the same range of log *K*-$\log(a_{TiO_2}/a_{Al_2O_3}^{0.5})$. Therefore, as expected, both the effects of fluid and of rock composition are important factors determining the composition of titanite. Because the slopes defined by the compositional variations of single samples in Figure 8 are very similar, it again appears that changes in *P* and *T* may not be the most important variables governing the Al and F content of the CDML titanites.

SUMMARY AND CONCLUSIONS

Titanite of varying Al and F contents in calcsilicates from Dronning Maud Land, Antarctica, formed at amphibolite- to granulite-facies conditions. The compositional variability in these titanites can be described by three linearly independent exchange vectors, one of which generates a vacancy. This hydroxylation was observed experimentally by Rosenberg (1974) in synthetic titanite and now can be confirmed for the first time in natural rocks.

Our observations indicate that the formation of high-Al titanite is possible under the whole range of geologically relevant *P-T* conditions, given high activities of HF in the coexisting fluid and low TiO_2/Al_2O_3 activity ratios in the host rocks. Because of the importance of coupled substitutions, high HF activities in the coexisting fluid alone are not able to enrich titanite in F, when a high TiO_2/Al_2O_3 activity ratio in the rock prohibits the incorporation of Al. On the other hand, low TiO_2/Al_2O_3 activity ratios can be accommodated for both by F or by OH incorporation and this exchange is thus relatively independent of fluid composition. These facts effectively rule out the easy use of titanite either as an indicator of fluid composition or as a thermobarometer as high-Al titanites

are expected to be common in skarns and calcsilicates formed under a wide range of *P-T* conditions.

Acknowledgments

We are grateful to Kurt Bucher, Universität Freiburg, and to the Bundesanstalt für Geowissenschaften und Rohstoffe, Hannover, for the possibility to take part in the German Antarctic Expedition GeoMaud 95/96, during which the samples of this study were collected. Constructive reviews by Jonathan Price, Darrell Henry, and an anonymous reviewer and comments by Bob Dymek improved this manuscript considerably and are gratefully acknowledged.

References cited

Andrehs, G. and Bormann, P. (1995) Metamorphics. Petermanns Geographische Mitteilungen, 287, 84–108.

Bernau, R. and Franz, G. (1987) Crystal chemistry and genesis of Nb-, V-, and Al-rich metamorphic titanite from Egypt and Greece. Canadian Mineralogist, 25, 695–705.

Bucher, K. and Ohta, Y. (1993) Granulites and garnet-cordierite gneisses from Dronning Maud Land, Antarctica. Journal of Metamorphic Geology, 11, 691–703.

Carswell, D.A., Wilson, R.N., and Zhai, M. (1996) Ultra-high pressure aluminous titanites in carbonate-bearing eclogites at Ahuanghe in Dabieshan, central China. Mineralogical Magazine, 60, 461–471.

Černý, P., Novak, M., and Chapman, R. (1995) The Al(Nb,Ta)Ti_{-2} substitution in titanite: the emergence of a new species? Mineralogy and Petrology, 52, 61–73.

Dalziel, I.W. (1991) Pacific margins of Laurentia and East Antarctica-Australia as a conjugate rift pair: Evidence and implications for an Eocambrian supercontinent. Geology, 19, 598–601.

Enami, M., Suzuki, K., Liou, J.G., and Bird, D.K. (1993) Al-Fe^{3+} and F-OH substitutions in titanite and constraints on their P-T dependence. European Journal of Mineralogy, 5, 219–231.

Franz, G. and Spear, F. (1985) Aluminous titanite (sphene) from the Eclogite-zone, south-central Tauern Window, Austria. Chemical Geology, 50, 33–46.

Gibert, F., Moine, B., and Gibert, P. (1990) Titanites (sphenes) alumineueses formees a basse/moyenne pression dans les gneiss a silicates calciques de la Montagne Noire. Comptes Rendus de l'Academie des Sciences Paris, serie II, 311, 657–663.

Jacobs, J., Fanning, C.M., Henjes-Kunst, F., Olesch, M., and Paech, H.J. (1998) Continuation of the Mozambique belt into East Antarctica: Grenville-age metamorphism and polyphase Pan-African high-grade events in central Dronning Maud Land. Journal of Geology, in press.

Kretz, R. (1983) Symbols for rock-forming minerals. American Mineralogist, 68, 277–279.

Markl, G. and Henjes-Kunst, F. (1999) Postkinematic charnockites in central Dronning Maud Land, Antarctica: self-retrogression of originally anhydrous rocks by late-magmatic fluids and modelling of their chemical, thermal and isotope evolution. Geologisches Jahrbuch, in press.

Markl, G. and Piazolo, S. (1998) Halogen-bearing minerals in syenites and high-grade marbles of Dronning Maud Land, Antarctica: monitors of fluid compositional changes during late-magmatic fluid-rock interaction processes. Contributions to Mineralogy and Petrology, 132, 246–268.

Munoz, J.L. and Swenson, A. (1981) Chloride-hydroxyl exchange in biotite and estimation of relative HCl/HF activities in hydrothermal fluids. Economic Geology, 76, 2212–2221.

Oberti, R., Smith, D.C., Rossi, G., and Caucia, F. (1991) The crystal-chemistry of high-aluminum titanites. European Journal of Mineralogy, 3, 777–792.

Piazolo, S. and Markl, G. (1999) Humite- and scapolite-bearing assemblages in marbles and calcsilicates of Dronning Maud Land, Antarctica and their implications on Gondwana reconstructions. Journal of Metamorphic Geology, in press.

Pouchou, J.L. and Pichior, F. (1984) A new model for quantitative analysis. I. Application to the analysis of homogeneous samples. La Recherche Aérospatiale, 3, 13–38.

Rao, D.R., Sharma, R., and Gururajan, N.S. (1997) Mafic granulites of the Schirmacher region, East Antarctica: fluid inclusion and geothermobarometric studies focusing on the Proterozoic evolution of the crust. Transactions of the Royal Society, Edinburgh, Earth Science, 88, 1–17.

Ribbe, P. (1982) Titanite. In Mineralogical Society of America Reviews in Mineralogy, 5, 137–154.

Rosenberg, P.E. (1974) Compositional variations in synthetic sphene. Geological Society of America Abstracts with Programs, 6, 1060.

Smith, D.C. (1981) The pressure and temperature dependence of Al-solubility in sphene in the system Ti-Al-Ca-Si-O-F. Progress of Experimental Petrology, Series D, 18, 193–197.

Manuscript received July 3, 1997
Manuscript accepted September 14, 1998
Paper handled by Gray E. Bebout

Appendix A: Sample locations and field relations

Sample 652 was collected at the eastern part of the central Konradberge. Here, an unzoned, up to 2 m thick calcsilicate unit is close to a charnockite body. GM 694, 695, 699, and 705 are from the nunatak Marmorny. GM 694 and 695 are from a massive clinopyroxene-fels, which contains centimeter-large spinel crystals. In most cases, these are surrounded by white corundum-margarite-anorthite-coronas (GM 695). GM 699 contains tschermakitic hornblende and considerable amounts of biotite in addition to abundant clinopyroxene. GM 705 was collected from a typical clinopyroxene-rich zone around a 1 m thick calcsilicate layer within a garnet-bearing gneiss. GM 799, 800, and 801 come from the nunatak Gjeruldsenhøgda, an area dominated by up to 2 km long strings of metasediments within an amphibole-bearing charnockite. The metasediments are interpreted as large xenoliths with thicknesses of 10 to 100 m. Often more than one calcsilicate layer of 1 to 5 m thickness occurs within these metasediments. Sometimes they are strongly zoned and boundinaged. The samples come from the rim and the middle part of such a boudin. GM 813 represents a calcsilicate boulder from the Schüssel moraine in northern Humboldtberge. Sample GM 859 is taken from a xenolith within the charnockite from the eastern part of the Eckhörner area in the northern Humboldtberge. GM 888 is a calcsilicate from an about 8 m wide layer within the metasedimentary sequence on Mt. Aerodromnaya in north-eastern Petermanberge. Here, no marble was associated with the calcsilicate. GM 919 comes from the eastern ridge of the ''Insel'' in northern Humboldtberge, where marbles and surrounding calcsilicates form abundant constituents within metapelitic gneisses. The particular sample GM 919 contains a large (3 cm) garnet crystal surrounded by a green amphibole-plagioclase symplectite against clinopyroxene. GM 941 was collected from an about 10 m thick calcsilicate layer at the main ridge in eastern Humboldtberge. Samples GM 951 and 952 are from the nunatak Odradnaya, which comprises a gabbro intrusion adjacent to metasediments. The samples are a few centimeters to decimeters thick layer within a few meters of the contact to the gabbro. GM 1035 is a sample from Lake Sbrosovoje in West Schirmacher Oasis. It borders a mafic gneiss and shows macroscopically large

grains of diopside, garnet, and quartz. In the entire Schirmacher Oasis, no forsterite-bearing marble was found.

Samples GM 967–1032 come from the steep slope southwest of Untersee in the Gruberberge. Here, 0.5–5 m thick calcsilicate rafts of up to a few tens of meters length are present within a ferrodiorite intrusion crosscutting anorthositic rocks. The calcsilicates are interpreted to be xenoliths of former marbles or calcsilicates that extensively reacted with the ferrodiorite. They consist exclusively of coarsely to giantly grained feldspars (both plagioclase and potassium feldspar), subcalcic augite and titanite. In most places, they are undeformed and not overprinted by later metamorphism. Titanite within these rocks forms euhedral crystals of variable size (0.1–6 cm) and layers of small anhedral grains. These layers reach a thickness of up to 0.5 m and lengths up to several tens of meters.